Towards an accurate description of anharmonic infrared spectra in solution within the polarizable continuum model: Reaction field, cavity field and nonequilibrium effects

Chiara Cappelli, Filippo Lipparini, Julien Bloino, and Vincenzo Barone

View Online　　**Export Citation**

ARTICLES YOU MAY BE INTERESTED IN

Towards an accurate description of anharmonic infrared spectra in solution within the polarizable continuum model: Reaction field, cavity field and nonequilibrium effects

Chiara Cappelli,[1,2,a)] Filippo Lipparini,[3] Julien Bloino,[3] and Vincenzo Barone[2,3]
[1]*Dipartimento di Chimica e Chimica Industriale, Università di Pisa, via Risorgimento, 35 I-56126 Pisa, Italy*
[2]*CNR–Consiglio Nazionale delle Ricerche, Istituto di Chimica dei Composti Organo Metallici (ICCOM-CNR), UOS di Pisa, Area della Ricerca, via G. Moruzzi 1, I-56124 Pisa, Italy*
[3]*Scuola Normale Superiore, Piazza dei Cavalieri, 7 I-56126 Pisa, Italy*

We present a newly developed and implemented methodology to perturbatively evaluate anharmonic vibrational frequencies and infrared (IR) intensities of solvated systems described by means of the polarizable continuum model (PCM). The essential aspects of the theoretical model and of the implementation are described and some numerical tests are shown, with special emphasis towards the evaluation of IR intensities, for which the quality of the present method is compared to other methodologies widely used in the literature. Proper account of an incomplete solvation regime in the treatment of the molecular vibration is also considered, as well as inclusion of the coupling between the solvent and the probing field (cavity field effects). In order to assess the quality of our approach, comparison with experimental findings is reported for selected cases. © *2011 American Institute of Physics*. [doi:10.1063/1.3630920]

I. INTRODUCTION

Effective *in silico* simulation of IR and Raman spectra for large systems in their natural environment is among the most significant tasks of contemporary theoretical and computational chemistry in view of the increasing reliability of the results coupled to the quite straightforward disentanglement of the role of different effects. However, the production of calculated spectroscopic data directly comparable to their experimental counterparts is particularly tricky in the case of solvated systems, that being mainly due to two reasons. First, the extraction of absolute data, especially intensity values, from spectra of solvated systems is far from being trivial, so that raw experimental values are often treated by means of some kind of theoretical assumptions (usually relying on classical theories) in order to extract from them the molecular property. Various examples exist in this context, especially in the field of nonlinear optical properties[1] and vibrational spectroscopies.[2–8] As a result, experimental data reported in the literature require careful analysis, i.e., any approximation and treatment of the data has to be taken into account if a direct comparison with absolute values is to be achieved. Second, from the purely theoretical and computational point of view, in order to obtain calculated values directly comparable to experiments, the models to be used should reliably represent the experimental sample, i.e., the physical model should be as realistic as possible, which in practice means that all the physical interactions in the sample and between the sample and the probing field have to be taken into account in the model.

The first implication of the previous statement is that a reliable description of the molecular system is needed. In the field of computational molecular spectroscopy, this almost always implies the use of quantum-mechanical (QM) methods to describe the system, since the electronic contribution is usually dominating. Of course, in case of solvated systems even the use of the most accurate QM method is meaningless if the role of the surrounding environment is neglected. Among the possible strategies which can be exploited to account for solvent effects on molecular properties and spectroscopies, a relevant role is played by continuum solvation models (CSM),[9] due to their well documented accuracy coupled to the relatively low computational cost, and the possibility to be coupled with different kinds of QM methodologies.[10–12] However, by even limiting ourselves to CSM, in order to get a reliable and quantitative description of the spectral features, the basic formulations which are generally exploited to model the energetics and the structural properties of molecular systems, have to be extended to treat effects which go beyond the direct solvent effect on the molecular wavefunction and its indirect effects on the molecular structure (the so-called reaction field effects).[13–15] Also, whether required on the basis of the chemical nature of the solute-solvent couple, combined discrete-continuum models, in which a few solvent molecules strongly and specifically interacting with the solute are treated explicitly leading to a sort of supermolecule embedded in a polarizable continuum, can be successfully employed.[16–19]

In the particular case of vibrational properties and spectroscopies, the harmonic oscillator/rigid rotor model has become a routine tool assisting in a very effective and general way the interpretation of spectroscopic experiments for isolated molecules, and is becoming a standard also in the case of solvated systems treated within CSMs, due to the development of analytical algorithms for the evaluation of

a)Author to whom correspondence should be addressed. Electronic mail: chiara@dcci.unipi.it.

energy second derivatives, which have proven to yield reasonably accurate results at reproducing the main features of vibrational spectra of systems in solution.[15,20] However, a purely harmonic description of the spectra poses serious accuracy issues in the reproduction of vibrational frequencies and intensities, as anharmonicity and vibro-rotational couplings come into play. Anharmonic effects also prevent the description of the whole vibrational spectrum since some spectral regions can be dominated by overtone transitions and combination bands. Methods for evaluating anharmonic effects on vibrational frequencies of solvated systems are still in their infancy, being to date limited to very few attempts reported in the literature,[21,22] including a recent paper by some of the present authors,[22] reporting on promising results, which retain both the accuracy and the scaling characteristics of the corresponding computations in vacuum. To the best of our knowledge, the QM evaluation of anharmonic IR intensities for solvated systems has never been treated before in the literature.

The evaluation of anharmonic terms by means of state-of-the-art electronic computations followed by converged variational solutions of the vibro-rotational problem provide nowadays very accurate results for small molecules (up to 5–6 atoms) in the gas phase. However, by even limiting the discussion to isolated systems, the extension of the anharmonic treatments to larger systems faces two major scaling problems. The first aspect concerns the building of the underlying potential energy surface (PES) and is being solved by linear scaling approaches[23] and, at least for localized enough vibrations, by multi-layer methods (e.g., ONIOM (Ref. 24)) in which different parts of the systems are treated at decreasing sophistication levels depending on the distance from the region to be described in detail. The PES is then expressed as a low-order (usually fourth) polynomial involving direct coupling of at most three independent coordinates. While this scheme presents several well-known limitations, especially when dealing with large amplitude low-frequency vibrations, it is computationally very effective and well sound for semi-rigid systems characterized by quite stiff and well separated energy minima. Starting from this point, perturbative and/or variational procedures can be used to solve the vibrational problem. Here we will be concerned with vibrational second order perturbation theory (VPT2),[25] which remains very attractive except for the presence of resonances which plague nearly all but the smallest systems. However, several studies are showing that, at least for low vibrational quantum numbers, resonances can be effectively treated either by small variational treatments of deperturbed polyads, or by more general perturbative developments.[25–27] When such models are coupled to electronic computations performed by hybrid (especially B3LYP)[28] or double hybrid (especially B2PLYP)[29] functionals and purposely tailored basis sets (e.g., N07D),[30] remarkably accurate vibrational frequencies and intensities can be obtained, which can be further improved by computing the harmonic part of the PES at a more advanced level.[31,32]

For the evaluation of anharmonic infrared (IR) intensities, after the pioneering work of Handy and co-workers,[33] a less cumbersome and simpler formula was proposed by Stanton and Vázquez,[34,35] who exploited the conventional Rayleigh-Schrödinger perturbation theory to take into account both electrical and mechanical anharmonicities. Recently, a fully automated implementation of VPT2 IR intensities has been proposed by some of the present authors[36] and a resonance-free version has been already implemented. On these grounds, we will report in the present contribution on the implementation and the first results of anharmonic computations of IR intensities in solution describing the response of the solvent by the polarizable continuum model (PCM).[9,37] This extension is by no means trivial since different time scales are involved in these computations, which require proper nonequilibrium models; at the same time, the "local field" acting on the solute is not the external field applied to the system, as it is the case for an isolated molecule.

In fact, from the conceptual point of view, in the case of a molecule surrounded by a dielectric, the probing radiation electric field acting on the molecule within a cavity immersed in the dielectric does not formally coincide with the field acting in the bulk of the dielectric (the so-called Maxwell field). There exists, therefore, a formal difference between the macroscopic spectroscopic response of the solution sample, which is defined in terms of the Maxwell field, and the response of the molecule in the cavity within a dielectric medium, which depends instead on the field locally acting on the molecule in the cavity. However, as already pointed out in the literature,[13–15,38–44] in order to gain a reliable connection between the microscopic properties of the molecule and the macroscopic response, it is compulsory to account for the difference between the Maxwell and the cavity fields.

In addition, due to the fact that spectroscopic properties are by definition time-dependent phenomena (due to the oscillatory nature of the radiation field), a time dependence is also to be accounted for in the definition of the solvation model. Here, formal differences exist depending on the nature of the spectroscopy under investigation; by limiting ourselves to IR spectroscopy, the time dependence of the radiation field is to be considered in the formulation of the cavity field, which is reflected in a proper definition of a the dielectric permittivity (*vide infra*). However, another implication is to be considered. In the case of an oscillatory motion caused by an external electric field on a molecule surrounded by a dielectric medium, the definition of the solvent response is different if it is assumed the solvent nuclear and electronic distributions to instantaneously rearrange to follow the oscillating molecule (vibrational equilibrium solvation regime), or if it is possible that there exists some dephasing between the solute and the solvent motions (vibrational nonequilibrum solvation regime), so that the solvent distribution is only partly equilibrated to the oscillating molecule. Such a problem has been previously discussed in the literature[39,45,46] for the PCM and will be re-considered here in the framework of anharmonic solute oscillations within the newest formalism proposed by Scalmani and Frisch[47] for the PCM. Note that the extension of the PCM to treat anharmonic IR frequencies has already been proposed by some of the present authors[22] within a purely equilibrium framework. The extension to a vibrational nonequilibrium solvation regime will be treated in Secs. II–III.

The paper is organized as follows. In Secs. II–III, the details on how to treat reaction field effects within the vibrational nonequilibrium solvation regime and cavity field effects for IR intensities will be given. After the derivation of the model to introduce such effects on a anharmonic description of IR intensities, application to a few small-sized selected model systems will be treated, so to separately evaluate the various sources of solvent effects on IR spectra. The focus will then be shifted to furan and phenol, for which a comparison of calculated and experimental results will also be reported. Some concluding remarks end the presentation.

II. VIBRATIONAL FREQUENCIES AND IR INTENSITIES: REACTION FIELD EFFECTS WITHIN THE VIBRATIONAL NONEQUILIBRIUM SOLVATION REGIME

The starting point for defining a solute-solvent system under the vibrational nonequilibrium solvation regime is the definition of the solvent polarization under nonequilibrium conditions. As it has already been amply reported in the literature,[9,48] the concept of a solute-solvent nonequilibrium system involves many different aspects, related to the real nature of the solvent polarization, which can formally be decomposed into different contributions, each related to the various degrees of freedom of the solvent molecules. On the other hand, each degree of freedom involves a different time scale. In the usual practice such contributions are grouped in two terms, the first one accounting for all the motions which are slower than those involved in the physical phenomenon under examination, and the second one defining the so-called fast contributions. By assuming only the latter to instantaneously equilibrate to the oscillating molecular charge distribution, the vibrational nonequilibrium solvation regime is defined as follows: the slow term accounts for the motions of the solvent molecules as a whole, i.e., translations and rotations, whereas the fast term takes into account the internal molecular motions, i.e., the electronic and vibrational solvent degrees of freedom. Following a shift from a previously reached equilibrium solute-solvent system, the fast polarization (which in the following will be defined through the dynamical (d) contributions to the polarization) is still in equilibrium with the new solute charge distribution but the slow polarization remains fixed at the value corresponding to the initial state solute charge distribution.

Within the PCM framework such a partition of the solvent polarization is done by formally defining two sets of polarization charges (or weights), the inertial charges, which remain fixed, and the dynamic (d) charges, which account for the time-dependent part of the solvent response and are defined through PCM equations depending on the dynamic dielectric constant. In the case of the vibrational nonequilibrium regime, in principle the dielectric constant at the vibrational frequency of interest should be used. However, when the solvent does not absorb at this frequency, it seems reasonable to approximate such a dielectric constant with the dielectric permittivity at optical frequencies, ε_{opt}.

As a further assumption, we will consider that the geometry of the molecular cavity does not follow the solute vibrational motion, which is consistent with the model we are exploiting, in which the solvent molecules are considered to be unable to rapidly rearrange their position and orientation around the perturbed solute.

More precisely, and by going into more details and using the notation introduced by Scalmani and Frisch,[47] the solvation regime just outlined implies to define a nonequilibrium free energy for the molecule in solution as[45,46]

$$\mathcal{G}_{neq} = \mathcal{G}_{vac} + \frac{1}{2}\mathbf{V}[\rho]q_d + \mathbf{V}[\rho]q_{in} - \frac{1}{2}\mathbf{V}[\rho^0]q_{in}, \qquad (1)$$

where ρ is the total density of charge (which takes into account both the nuclei and the electrons) of the solute at a given nuclear configuration and is in general different from the equilibrium one ρ^0. $\mathbf{V}$ is the electrostatic potential due to the solute at the surface points i (N is the number of atoms):

$$V_i = \sum_{A=1}^{N} Z_A \langle i|A\rangle - \sum_{\mu\nu} \mathbf{P}_{\mu\mu} \langle i|\mu\nu\rangle. \qquad (2)$$

The two sets of polarization charges in Eq. (1) are

$$q_d = -\mathbf{U}(\varepsilon_\infty)\mathbf{V},$$

$$q_{in} = q - q_d,$$

where

$$q = -\mathbf{U}(\varepsilon)\mathbf{V},$$

are the equilibrium polarization charges. The $\mathbf{U}(\varepsilon)$ matrix is the PCM response matrix, whose mathematical definition depends on the particular PCM version chosen,[9] and is defined in terms of the solvent dielectric permittivity, which, as already commented above, is set to the optical value to calculate the dynamic d charges.

As reported in the original paper,[45] the gradient of the nonequilibrium free energy at the equilibrium geometry is equal to the fixed-cavity equilibrium free energy gradient at the same geometry, so that further geometry optimization is not required.

Moving to nonequilibrium free energy second derivative, by keeping the formalism of Refs. 49 and 50, we obtain (more details are reported in the Appendix):

$$\mathcal{G}[\rho]_{neq}^{xy} = \mathcal{G}_{neq}^{xy}[\rho^0] + tr\mathbf{P}^x\tilde{\mathbf{F}}^y[\rho^0] - tr\mathbf{S}^{xy}\tilde{\mathbf{W}} - tr\mathbf{S}^x\mathbf{W}^y, \qquad (3)$$

$\mathbf{S}$ is the overlap matrix, $\tilde{\mathbf{W}} = \mathbf{R}\tilde{\mathbf{F}}\mathbf{R}$ (with $\mathbf{R}$ being the density matrix) and the derivatives of the energy evaluated at the equilibrium density are

$$\mathcal{G}_{neq}^{xy}[\rho^0] = \frac{1}{2}\mathbf{V}^{xy}q + \frac{1}{2}\mathbf{V}q^{xy} + \mathbf{V}^x q_d^y = \mathbf{V}^{xy}q + \mathbf{V}^x q_d^y, \qquad (4)$$

In Eq. (4) the charges might be replaced by polarization weights, depending on the PCM fashion adopted.[51,52] If we assume the cavity to be fixed at the equilibrium geometry, the

derivatives of the charges are obtained as

$$q^x = -\mathbf{U}\mathbf{V}^x.$$

The Fock operator derivative in Eq. (3) is

$$\tilde{\mathbf{F}}^y(\rho) = \tilde{\mathbf{F}}^y(\rho^0) + \tilde{\mathbf{G}}(\mathbf{P}^y), \tag{5}$$

where $\tilde{\mathbf{G}}(\mathbf{P}^y)$ is the bielectronic component of the PCM-Fock operator. The nonequilibrium PCM contribution to the explicit derivative of the Fock matrix is

$$\mathbf{X}_{\mu\nu}^y = \mathbf{V}_{\mu\nu}^y q + \mathbf{V}_{\mu\nu} q_d^y. \tag{6}$$

The modified Fock operator derivative in Eq. (5) is also used to obtain the nonequilibrium density matrix derivatives $\mathbf{P}^y$ through the solution of the proper Coupled-Perturbed Hatree-Fock (or Kohn-Sham) CPHF (CPKS) set of equations for the solvated system.[53] Note that, as it has already been pointed out in a previous work of some of the present authors,[22] in order to be able to reliably compute anharmonic vibrational frequencies and intensities in solution via further numerical differentiation of analytical geometric second derivatives, a formulation of PCM in a continuous surface charge formalism[47] is required.

A. Vibrational intensities: Cavity field effects

By following Ref. 13, IR intensities for solvated systems taking into account both reaction and cavity field effects (and possibly vibrational nonequilibrium) can be calculated by exploiting the usual formula, i.e.,

$$I_v^{sol} = \frac{\pi \mathcal{N}_A}{3c^2 n_s} v_v g_v \sum_\alpha |\langle 0 \mid \bar{\boldsymbol{\mu}}^\alpha \mid v \rangle|^2 (N_0 - N_v), \tag{7}$$

where $\mathcal{N}_A$ is the Avogadro number, n_s the refractive index of the solution and g_v and N_v are the degeneration and the Boltzmann population of the vibrational state $|v\rangle$, respectively. In the following, however, the population of the excited states will be considered negligible.

$\bar{\boldsymbol{\mu}}$ is the so-called "effective" dipole moment for the solvated system defined according to the previous literature:[13–15,38–43,54,55]

$$\bar{\boldsymbol{\mu}} = \boldsymbol{\mu} + \tilde{\boldsymbol{\mu}}, \tag{8}$$

where $\boldsymbol{\mu}$ is the electric dipole operator and $\tilde{\boldsymbol{\mu}}$ is the operator which accounts for the differences between the cavity and Maxwell fields, and which in the PCM is expressed in terms of the apparent charges produced by the Maxwell field on the cavity, i.e.,

$$\tilde{\boldsymbol{\mu}} = \sum_l V(\mathbf{s}_l) \frac{\partial q_l^{ex}}{\partial \mathbf{E}^M}. \tag{9}$$

The potential terms $V(\mathbf{s}_l)$ come from the molecular electronic potential evaluated at cavity representative points and the so-called external surface charges q_l^{ex} describe the dielectric polarization in response to the external field $\mathbf{E}$. In particular,

$$\mathbf{q}^{ex} = -\mathbf{D}^{-1}\mathbf{e}_n^M, \tag{10}$$

where $\mathbf{D}^{-1}$ is a dielectric PCM-type solvent response matrix which describes the solvent polarization with respect to a perturbing electric field, and $\mathbf{e}_n^M$ is a vector collecting the normal

components of the Maxwell field $\mathbf{E}^M$ at the center of each representative point (l) of the cavity.

Notice that, as already pointed out in Ref. 13, the dependence of I_v^{sol} in Eq. (7) on the refractive index n_s of the solution under study follows from the relation between the intensity I of the radiation and the Maxwell electric field $\mathbf{F}^M$ in solution,[56] namely:

$$I = \frac{\varepsilon_s c}{2\pi n_s}(\mathbf{F}^M)^2 \approx \frac{n_s c}{2\pi}(\mathbf{F}^M)^2, \tag{11}$$

where it is assumed that the dielectric constant of the solution ε_s is equal to square of the refractive index n_s^2. This corresponds to the assumption that the magnetic permittivity of the medium is roughly equal to 1. Note that in the following, infinitely dilute solutions will be considered, so that the refractive index will be set to that of the pure solvent. We recall here that in the calculation of the PCM matrix (Eq. (10)) and in Eq. (7), the dielectric permittivity and refractive index at the frequency of interest should be used. In this work, as already done in other previous studies[13,14,39,40,44,49] the optical values are used. Also, the use of a non-zero field dielectric permittivity takes into account the oscillatory nature of the external probing field.

III. ANHARMONIC IR INTENSITIES IN SOLUTION: SECOND-ORDER PERTURBATIVE EXPRESSION FOR VIBRATIONAL TRANSITION DIPOLES

In this section, we will extend the treatment outlined above to the calculation of anharmonic IR intensities. The formulation of anharmonic frequencies within the vibrational nonequilibrium solvation regime will not be explicitly treated. In fact, the numerical evaluation of anharmonic contributions in the perturbative formalism[27,57] requires the numerical differentiation of the nonequilibrium free energy derivatives in Eq. (3) with respect to nonequilibrium normal modes obtained through the diagonalization of the Hessian matrix obtained by means of the same quantities, similarly to what has already been reported in the literature.[22] It is worth spending, instead some more words regarding the formulation of anharmonic IR intensities in the nonequilibrium solvation regime with the further account of local field effects.

We keep exactly the same formalism used in Ref. 36 to represent the nth derivative of the "effective" dipole moment $\bar{\boldsymbol{\mu}}$ for the solvated systems ($\bar{\boldsymbol{\mu}}_{ijk...}$) and of the potential energy V^{sol} in solution ($\Phi_{ijk...}^{sol}$) with respect to the normal modes $q_i^{sol}, q_j^{sol}, q_k^{sol}, \ldots$ calculated at the equilibrium geometry e. Within the PCM formalism, they are ($\{q_1^{sol} \ldots q_N^{sol}\}$ is the set of the N dimensionless reduced normal coordinates of the system calculated in solution, by accounting of reaction field effects in the vibrational nonequilibrium regime):

$$\bar{\boldsymbol{\mu}}_{ijk...} = \left(\frac{\partial^n \bar{\boldsymbol{\mu}}}{\partial q_i^{sol} \partial q_j^{sol} \partial q_k^{sol}...}\right)_e, \tag{12}$$

$$\Phi_{ijk...}^{sol} = \left(\frac{\partial^n V^{sol}}{\partial q_i^{sol} \partial q_j^{sol} \partial q_k^{sol}...}\right)_e. \tag{13}$$

In the following, $\bar{\boldsymbol{\mu}}^\alpha$ and $\bar{\boldsymbol{\mu}}_{ijk...}^\alpha$ refer to any Cartesian component α of the vectors $\bar{\boldsymbol{\mu}}$ and $\bar{\boldsymbol{\mu}}_{ijk...}$; B_e^γ is the diagonal inertia

tensor of the molecule at the equilibrium geometry and ζ_{ij}^{γ} are the Coriolis zeta constants coupling the modes i and j along the rotation axis I_{γ}. The potential energy, the frequencies and the inertia tensor components are expressed in cm^{-1} and the

dipole moment in Debye. With that notation, the transition dipole relative to the fundamental bands for the solvated systems, with the account of reaction field, cavity field and vibrational nonequilibrium effects reads:

$$
\begin{aligned}
\langle \bar{\boldsymbol{\mu}}^{\alpha} \rangle_{0i} =\ & \frac{1}{\sqrt{2}} \bar{\boldsymbol{\mu}}_i^{\alpha} + \frac{1}{4\sqrt{2}} \sum_j \bar{\boldsymbol{\mu}}_{ijj}^{\alpha} - \frac{1}{8\sqrt{2}} \sum_{jk} \left[\left(\frac{1}{\omega_i+\omega_j+\omega_k} - \frac{1}{\omega_i-\omega_j-\omega_k} \right) \Phi_{ijk}^{sol} \bar{\boldsymbol{\mu}}_{jk}^{\alpha} + \frac{2}{\omega_k} \Phi_{kjj}^{sol} \bar{\boldsymbol{\mu}}_{ik}^{\alpha} \right] \\
& + \frac{1}{16\sqrt{2}} \sum_{jkl} \left\{ \Phi_{ikl}^{sol}\Phi_{jkl}^{sol} \bar{\boldsymbol{\mu}}_j^{\alpha} \left[\frac{4\omega_j(\omega_l+\omega_k)(1-\delta_{ij})(1-\delta_{ik})(1-\delta_{il})}{(\omega_i^2-\omega_j^2)[\omega_i^2-(\omega_l+\omega_k)^2]} - \frac{(\omega_l+\omega_k)[3\omega_i^2-(\omega_l+\omega_k)^2]\delta_{ij}(1+\delta_{ik})(1-\delta_{il})}{\omega_i[\omega_i^2-(\omega_l+\omega_k)^2]} \right. \right. \\
& \left. - \frac{4\omega_j(7\omega_i\omega_k+3\omega_k\omega_j+3\omega_k^2+4\omega_i\omega_j+4\omega_i^2)(1-\delta_{ij})(1-\delta_{ik})\delta_{il}}{\omega_k(2\omega_i+\omega_k)(\omega_i^2-\omega_j^2)(\omega_i+\omega_j+\omega_k)} \right] + \Phi_{ijk}^{sol}\Phi_{llk}^{sol} \bar{\boldsymbol{\mu}}_j^{\alpha} \left[\frac{\delta_{ij}}{\omega_i\omega_k} \left(1 + \frac{2}{9}\delta_{ik}\delta_{il} \right) \right. \\
& \left. \left. - \frac{4\omega_j(1-\delta_{ij})(1-\delta_{ik})(1-\delta_{il})}{\omega_k(\omega_i^2-\omega_j^2)} - \frac{4\omega_j\delta_{ik}(1-\delta_{ij})}{\omega_i(\omega_i^2-\omega_j^2)} \left(1 + \frac{2}{3}\delta_{il} \right) \right] \right\} - \frac{1}{8\sqrt{2}} \sum_{jk} \Phi_{ijkk}^{sol} \bar{\boldsymbol{\mu}}_j^{\alpha} \left(\frac{1}{\omega_i+\omega_j} - \frac{1-\delta_{ij}}{\omega_i-\omega_j} \right) \\
& + \frac{1}{2\sqrt{2}} \sum_{jk \neq i} \left\{ \sum_{\tau=x,y,z} B_e^{\tau} \zeta_{ij}^{\tau} \zeta_{jk}^{\tau} \left[\frac{\sqrt{\omega_i\omega_k}}{\omega_j} \left(\frac{1}{\omega_i+\omega_k} + \frac{1-\delta_{ik}}{\omega_i-\omega_k} \right) - \frac{\omega_j}{\sqrt{\omega_i\omega_k}} \left(\frac{1}{\omega_i+\omega_k} - \frac{1-\delta_{ik}}{\omega_i-\omega_k} \right) \right] \bar{\boldsymbol{\mu}}_k^{\alpha} \right\}.
\end{aligned} \tag{14}
$$

In the previous equation, all the ω values are to be considered for the solvated system, i.e., they account for both reaction field and nonequilibrium effects. The B term is diagonal, i.e.,

$$
\sum_{\tau,\alpha=x,y,z} B_e^{\tau\alpha} \zeta_{ij}^{\tau} \zeta_{jk}^{\alpha} = \sum_{\tau=x,y,z} B_e^{\tau} \zeta_{ij}^{\tau} \zeta_{jk}^{\tau}.
$$

In the case of overtones up to two quanta ($\langle 0 \mid \bar{\boldsymbol{\mu}}^{\alpha} \mid 0+2v_i \rangle$) and combination bands of two singly excited modes ($\langle 0 \mid \bar{\boldsymbol{\mu}}^{\alpha} \mid 0+v_i+v_j \rangle$), we have

$$
\begin{aligned}
& \langle \bar{\boldsymbol{\mu}}^{\alpha} \rangle_{0,i(1+\delta_{ij})+j(1-\delta_{ij})} \\
& = \left(1 + \frac{(1-\sqrt{2})\delta_{ij}}{\sqrt{2}} \right) \left(\frac{1}{2} \bar{\boldsymbol{\mu}}_{ij}^{\alpha} + \frac{1}{4} \sum_k \Phi_{ijk}^{sol} \bar{\boldsymbol{\mu}}_k^{\alpha} \right. \\
& \left. \times \left(\frac{1}{\omega_i+\omega_j-\omega_k} - \frac{1}{\omega_i+\omega_j+\omega_k} \right) \right),
\end{aligned} \tag{15}
$$

The first derivatives of $\bar{\boldsymbol{\mu}}$ with respect to the nuclear coordinates, $\bar{\boldsymbol{\mu}}_i$, are obtained analytically as

$$
\bar{\boldsymbol{\mu}}_i^{\alpha} = \frac{\partial \bar{\boldsymbol{\mu}}^{\alpha}}{\partial q_i} = -tr\left[\mathbf{P}^i \bar{\mathbf{m}}^{\alpha} + \mathbf{P}\bar{\mathbf{m}}_i^{\alpha} \right] + \bar{\boldsymbol{\mu}}_i^{N,\alpha}. \tag{16}
$$

$\mathbf{P}$ and $\mathbf{P}^i$ are the density matrix and density matrix derivatives with respect to q_i, respectively. The latter accounts for vibrational nonequilibrium effects, being obtained by exploiting the nonequilibrium Fock operator derivative (see Eq. (5)). $\bar{\mathbf{m}}_i^{\alpha}$ is the derivative of the "effective" dipole matrix $\bar{\mathbf{m}}^{\alpha}$ with respect to q_i, and thus accounts for cavity field effects (see Sec. II A). Its expression, which can be found in Ref. 13, can be written as a sum of two contributions: the first one arises from the dependence of the basis functions on the nuclear positions and the other is due to the dependence of the cavity geometry on the nuclear geometry, which is discarded in the

present case, following our model for vibrational nonequilibrium effects. Finally, $\bar{\boldsymbol{\mu}}_i^{N,\alpha}$ is the nuclear term.

The $\bar{\boldsymbol{\mu}}_{ij}$ and $\bar{\boldsymbol{\mu}}_{ijj}$ terms in Eq. (14), which correspond to the first and second derivatives of Eq. (16), are obtained through numerical first and second differentiation. The Φ_{jkl}^{sol} and Φ_{ijkk}^{sol} are obtained as well by numerical differentiation of the nonequilibrium free energy second derivatives in Eq. (4), from which also the ω values are calculated.

We remark that the previous treatment of anharmonic intensities strictly implies the absence of any frequency resonance. In case of resonance, in fact, divergence occurs due to the presence of frequency differences in the denominators of Eq. (14). Extension of the treatment to resonances is possible and is currently under development at our laboratory. Further details will be presented in a following communication.

IV. NUMERICAL RESULTS

A. Computational details

The calculation of anharmonic frequencies and intensities in the nonequilibrium solvation regime was implemented in a locally modified version of the GAUSSIAN 09 (G09) (Ref. 58) suite of programs, by extending to the IEF version[59] of the PCM the existing code to calculate frequencies and force constants at the same level of theory[27] for isolated systems. According to Ref. 36, the calculations for H_2O, C_2H_2, CH_2F_2, SiH_2Cl_2, H_2O_2, F_2NO, and the vinyl radical were performed at the B3LYP/aug-cc-pVTZ level, whereas the B3LYP/N07Ddiff (Ref. 60) level was used for furan and phenol. Pruned grids (75, 302) and (50, 194) were exploited for the evaluation of energies and energy derivatives, and in the CPKS, respectively. In the case of phenol, most of the

calculations were performed by treating anharmonically only the O–H stretching normal coordinate in the perturbative framework, that in order to decrease the computational cost. Note that this does not mean to consider only one-dimensional anharmonicity along the OH normal mode, since the Hessian numerical differentiation provides all the couplings between OH and all normal modes except for some usually small contributions.[61] In the numerical differentiation, a stepsize of 0.025 Å was exploited, which was chosen according to previous studies.[27] In the lack of resonances, the stepsize is the only adjustable parameter used to set up anharmonic calculations.

The IEF-PCM calculations in cyclohexane and acetone for H_2O, C_2H_2, CH_2F_2, SiH_2Cl_2, H_2O_2, F_2NO, the vinyl radical, and furan were done by using G09 default settings to define the solvent dielectric constants and refractive index, as well as the cavity shape and size. In particular, for each molecule, the cavity is defined as the results of the interlocking of one sphere centered on each atom, each having the following radii (the $\alpha = 1.1$ scaling factor is already included in the values): C:2.1175 Å; H: 1.5873Å; O: 1.925 Å; F: 1.8502 Å; Si: 2.3628 Å; Cl: 2.1714 Å; N: 2.013 Å. The following values were used for the dielectric parameters: cyclohexane: $\varepsilon = 2.0165$ and $n^2 = 2.035188$; acetone $\varepsilon = 20.493$ and $n^2 = 1.846337$.

The calculations for phenol were performed by setting the dielectric constants of cyclopentane, CCl_2, tetrachloroethylene and CS_2 to G09 default settings (i.e., $\varepsilon = 1.9608$ for cyclopentane, $\varepsilon = 2.228$ for CCl_2, $\varepsilon = 2.268$ for tetrachloroethylene and $\varepsilon = 2.6105$ for CS_2). For 2,2-dimethylbutane $\varepsilon = 1.843$ was used, according to the value reported in Ref. [62] for 2-methylbutane. The refractive indexes of all the previously mentioned solvents were set according to Ref. [63] and used to calculate the PCM matrices involved in the definition of the "effective" properties and in the calculation of the second derivatives within the nonequilibrium regime. The cavity size for phenol was varied in order to evaluate the differences in the description arising from the cavity definition. Besides the use of G09 default settings, a user-defined cavity constituted by 8 spheres was also considered, by setting the following radii values: CH = 2.0 Å, O = 1.52 Å, H = 1.2 Å. The sphere on hydrogen was multiplied by a varying α scaling factor (see tables), whereas $\alpha = 1.2$ was set for all the other spheres. In all cases, no added spheres were considered in the definition of the molecular cavity, as proposed in Refs. [47] and [64]. The solute geometry was optimized with each cavity.

The spectra reported in Figs. [5] and [7] were obtained by broadening each calculated transition by means of a Lorentzian lineshape function with 10 cm^{-1} width at half maximum.

B. Solvent effects on vibrational anharmonic IR intensities of model molecules: Benchmarking with respect to classical theories

A traditional way to rationalize solvent effects on vibrational intensities is to resort to classical solvation theories for expressing the ratio between the band intensity of the solvated

system I_{sol} and the corresponding one for the isolated system, I_{sol}/I_{vac}. Among such a class of theories, the most exploited method is probably the one proposed by Polo and Wilson:[2]

$$\left(\frac{I_{sol}}{I_{vac}}\right)_{PW} = \frac{1}{n}\left(\frac{n^2+2}{3}\right)^2. \qquad (17)$$

Such an equation is rigorously applicable to pure liquids, but can easily be extended to solutions, giving origin to the Mallard-Straley[3] and Person[4] equation; however, in the limit of infinitely dilute solutions, the two equations coincide.[13]

Other formulations of the I_{sol}/I_{vac} ratio exist, such as the one proposed by Hirota:[5]

$$\left(\frac{I_{sol}}{I_{vac}}\right)_H = \left[\frac{(n^2+2)(2\varepsilon+1)}{3(n^2+2\varepsilon)}\right]^2,$$

or by Buckingham:[6]

$$\left(\frac{I_{sol}}{I_{vac}}\right)_B = \left[\frac{9\varepsilon_{opt}}{(\varepsilon_{opt}+2)(2\varepsilon_{opt}+1)}\right]^2\left[\frac{(n^2+2)(2\varepsilon+1)}{3(n^2+2\varepsilon)}\right]^2.$$

The previous equations are generally rooted into the Onsager's theory of dielectric polarization[65,66] and assume a continuous description of the environment and a classical picture of the molecular system, which is assimilated to a polarizable point dipole in a large spherical cavity in the dielectric.

The comparison between PCM harmonic IR intensities and the classical theories has been previously shown in Ref. [13]. Here, we will carry out the same comparison for anharmonic values obtained through Eq. (7) by exploiting the transition dipoles defined in Eqs. (14) and (15). The results are pictorially shown in Fig. 1 for the seven model molecules investigated here and immersed in a non-polar solvent (cyclohexane) and in a polar one (acetone). Note that the calculated values in solution were obtained by exploiting the full nonequilibrium + cavity field model.

In most cases the classical equations only roughly approximate the calculated ratios, and the overall quality of the three different classical approaches is almost the same. More notably, calculated PCM ratios depend on the normal mode under investigation, i.e., depend on the nature of the molecule and how its geometrical and electronic properties change upon vibration. In the classical theories, however, no dependence on the molecule exists, so that the ratio only depends on the dielectric properties of the solvent and for a given solvent stays the same irrespective of the nature and shape of the molecular system, which is simply seen as an oscillating point dipole. The I_{sol}/I_{vac} ratio, which by definition accounts for both reaction and cavity field contributions, strongly depends on the level of approximation which is used to model both effects, and the final comparison between the classical and QM methodologies is a balance of the different levels of approximation exploited.

In the case of PCM solutes, the molecule is a quantum system and its structure and vibrational properties (vibrational transition moments) are obtained with quantum-mechanical techniques. The level of treatment of reaction field effects is not easy to be extracted in the classical theories. In fact, in the case of continuum solvation
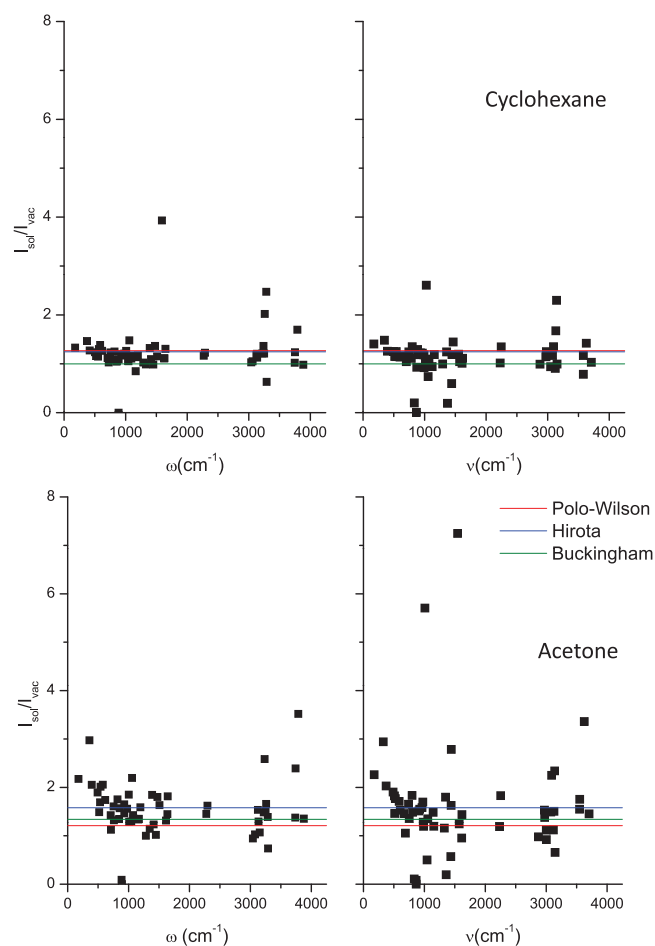
FIG. 1. Calculated PCM local field factors for the various systems investigated here as a function of the frequency of the band. Harmonic (left) and anharmonic (right), computed in cyclohexane and acetone. The solid lines give the values obtained through the classical theories (see text).

theories such effects, which are still present in the case of the non-vibrating molecular system immersed in the medium, are modeled in terms of the solvent static dielectric permittivity ε. Among the three classical theories mentioned above, those devised by Hirota and Buckingham explicitly account for reaction field effects through the ε parameter, whereas the Polo-Wilson approach is only focused on the screening of the external oscillating electric field due to the presence of the solvent (such effects are also considered in both Hirota and Buckingham approaches). Despite such a fundamental difference, the quality of the reproduction of the PCM data is almost the same, this being reasonably due to the fact that the actual shape of the molecular cavity in the case of PCM is generally far from being approximable by a single sphere, so that the consideration of reaction field effects for a spherical cavity badly describes the effects when the cavity considerably deviates from a sphere. Figure 2 illustrates such concepts in more details, by focusing the comparison on two specific cases, i.e., NOF$_2$ and furan, whose PCM molecular cavities are the most similar (NOF$_2$) and the most different (furan) from a single sphere. For NOF$_2$, the scattering of the values around the classical values is less pronounced than for furan. Also, the approximation of the QM data with the classical data seems to be more reasonable for the nonpolar solvent (cyclo-

hexane), whereas in acetone the deviation is larger, even in the case of NOF$_2$, this being presumably due to the fact that the solvent effect in cyclohexane is less pronounced than in acetone, so that the rough classical approximation works better in the first case. Note that all PCM data reported here were obtained by also considering nonequilibrium effects, which in the classical approaches appear to be considered by the Buckingham approach only, at least to some extent, due to the dependence of the equation on the ε_{opt} parameter.

Another level of analysis consists in focusing on cavity field effects only, i.e., to extract from the calculated data the ratio between intensity values obtained by discarding or including the cavity field correction (see Sec. II A). By extending the Onsager-Lorentz theory to IR intensities, the following quantity is obtained:[13]

$$f_{Ons}^{CF} = \left(\frac{3\varepsilon_{opt}}{2\varepsilon_{opt} + 1} \right)^2. \tag{18}$$

The comparison between PCM data and the classical equation is shown in Fig. 3 for the same set of molecules as above. The quality of the comparison is basically the same as already commented for the whole "local field" effect. Also in this case a strong dependence upon the shape of the molecular cavity is observed, which is illustrated by the plots reported in Fig. 4.

C. The IR anharmonic spectrum of furan in acetone: Equilibrium vs nonequilibrium

In this section, the attention will be focused on the evaluation of the effects arising from the assumption of a nonequilibrium regime. In Fig. 5 calculated harmonic and anharmonic IR spectra of furan in acetone are reported, within both equilibrium and nonequilibrium solvation regimes.

Generally, the shift in the peak maxima between the two approaches is more marked in the case of anharmonic spectra, but it also strongly depends not only on the specific system but especially on the normal mode. Therefore, the findings previously reported in the literature[45] regarding the small effect of vibrational nonequilibrium on harmonic vibrational frequencies in the case of the carbonyl stretching mode of a series of ketones does not seem to generally occur.

Regarding the relative intensities of the peaks, the differences between equilibrium and nonequilibrium observed here are in line with previous findings,[45] with more pronounced effects in the anharmonic case. However, a general trend cannot be evidenced, due to the normal mode specific behavior identified from the observation of Fig. 5. The effects mentioned here are stronger for anharmonicity, because of not only the presence of overtone and combination bands but also a variation of fundamental band intensities as a result of the anharmonic treatment of IR intensities. Such a behavior can be relevant especially in case calculated spectra are to be exploited for peak assignment.

In order to compare calculated and experimental data, the experimental IR spectrum of pure liquid furan is also reported in Fig. 5. As expected anharmonic calculated spectra are overall more similar to the experiment, this being mainly due to
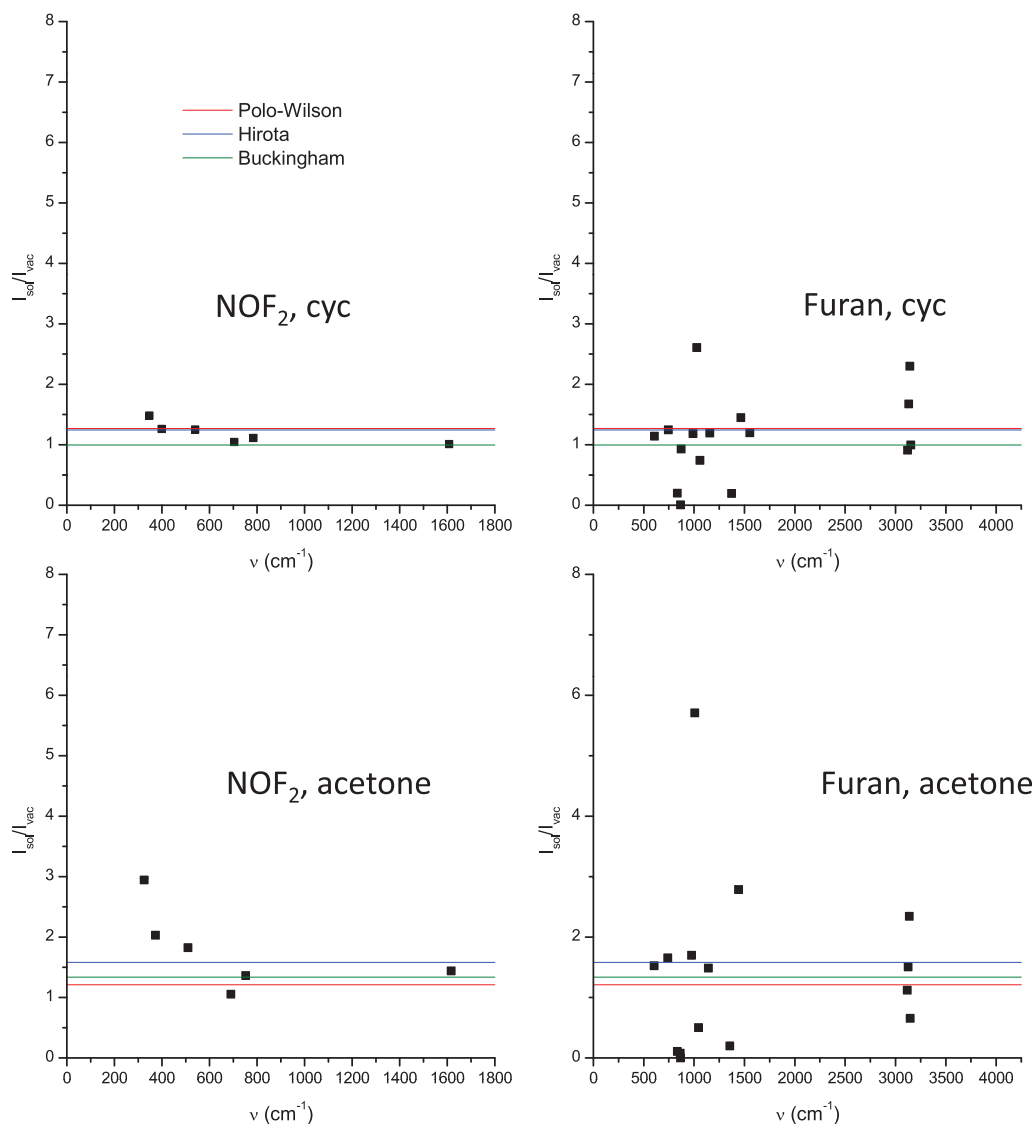
FIG. 2. Calculated PCM local field factors for NOF$_2$ and furan as a function of the frequency of the band. Data refer to anharmonic values, in cyclohexane (cyc) and acetone. The solid lines give the values obtained through the classical theories (see text).

the appearance of overtones and combination bands in the region between 2000 and 2700 cm^{-1}. A clear assessment of the quality of the two approaches at reproducing the experiments is not easy to make in this case, both being very good at reproducing fundamental bands. In fact, as far as the reproduction of experimental frequencies is concerned, they perform very similarly (see Fig. 6). However, a frequency shift between the two approaches is visible, and as already pointed out before, this can be an issue if calculations are to be exploited for experimental band assignment. Also, larger differences are noticed for peak relative intensities, which cause the whole spectrum to change its appearance as a function of the solvation regime employed.

D. The O–H stretching mode of phenol: Solvent effects on band intensities

   In this section, we will focus more specifically on the ability of our full anharmonic nonequilibrium + local field approach to reproduce solvent effects on band intensities. To

this end, a strongly anharmonic vibration was selected, i.e., the O–H stretching mode of phenol. The combined effects of pressure and solvents on the O–H stretching mode of phenol have been investigated by Isogai *et al.*,[63] who have also studied quantitatively the effects of the solvent on absorption intensities. They also further tested the results against the Polo-Wilson approach, obtaining unsatisfactory results, so that the present case appears to be ideal to test our refined model.

   Before commenting on O–H stretching mode intensities, we will discuss the overall performance of our methodology to reproduce the entire IR spectrum. In Fig. 7, the calculated anharmonic IR spectrum of phenol in carbon disulfide is reported. To assist the comparison, the experimental IR spectrum of phenol is also reported. Notice that experiments were performed on a 10% solution in CCl$_2$ (3800–1300 cm^{-1} and 650–250 cm^{-1}) and in CS$_2$ (1300–650 cm^{-1}). Although our calculations were performed on CS$_2$ over the entire range, the dielectric properties of the two solvents used in the experiment are sufficiently similar (CCl$_2$: $\varepsilon = 2.2280$, $n^2 = 2.1319$;
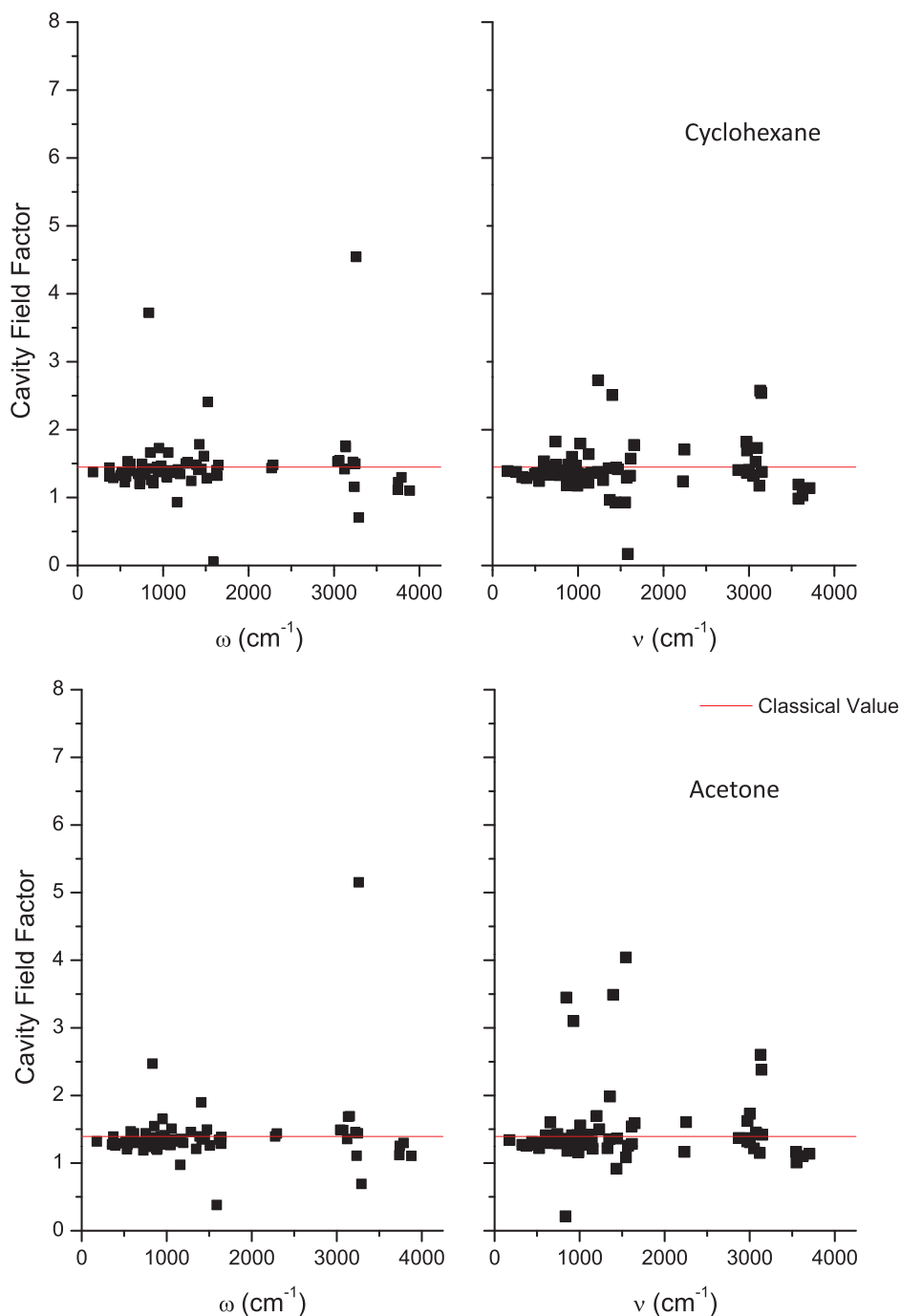
FIG. 3. Calculated PCM cavity field factors for the various systems here investigated as a function of the frequency of the band. Harmonic (left) and anharmonic (right), computed in cyclohexane and acetone. The classical values of the factors are represented by the solid red lines.

CS_2: $\varepsilon = 2.6105$, $n^2 = 2.6631$) to justify the qualitative comparability between the calculations and the experimental findings. The sample was also, as declared by experimentalists, contaminated by water. Overall, the reproduction of the spectral patterns is very good, both in terms of frequency values and peaks relative intensities.

Going into more details, anharmonic frequencies and IR intensities of the O–H stretching mode of Phenol in various solvents are reported and compared with experimental findings[63] (Tables I and II). The corresponding data obtained

within the double harmonic approximation are given as supplementary material.[69]

As far as solvation is concerned, equilibrium (*eq*) and nonequilibrium (*neq*) solvation are compared. All intensity values account for cavity field effects. Also, since the only really adjustable parameter in PCM calculations besides the setting of the solvent dielectric parameters are the cavity shape and size, in order to evaluate the range of variability of our results as a function of such parameters, in the columns labeled with the α values, we report the data obtained by keeping
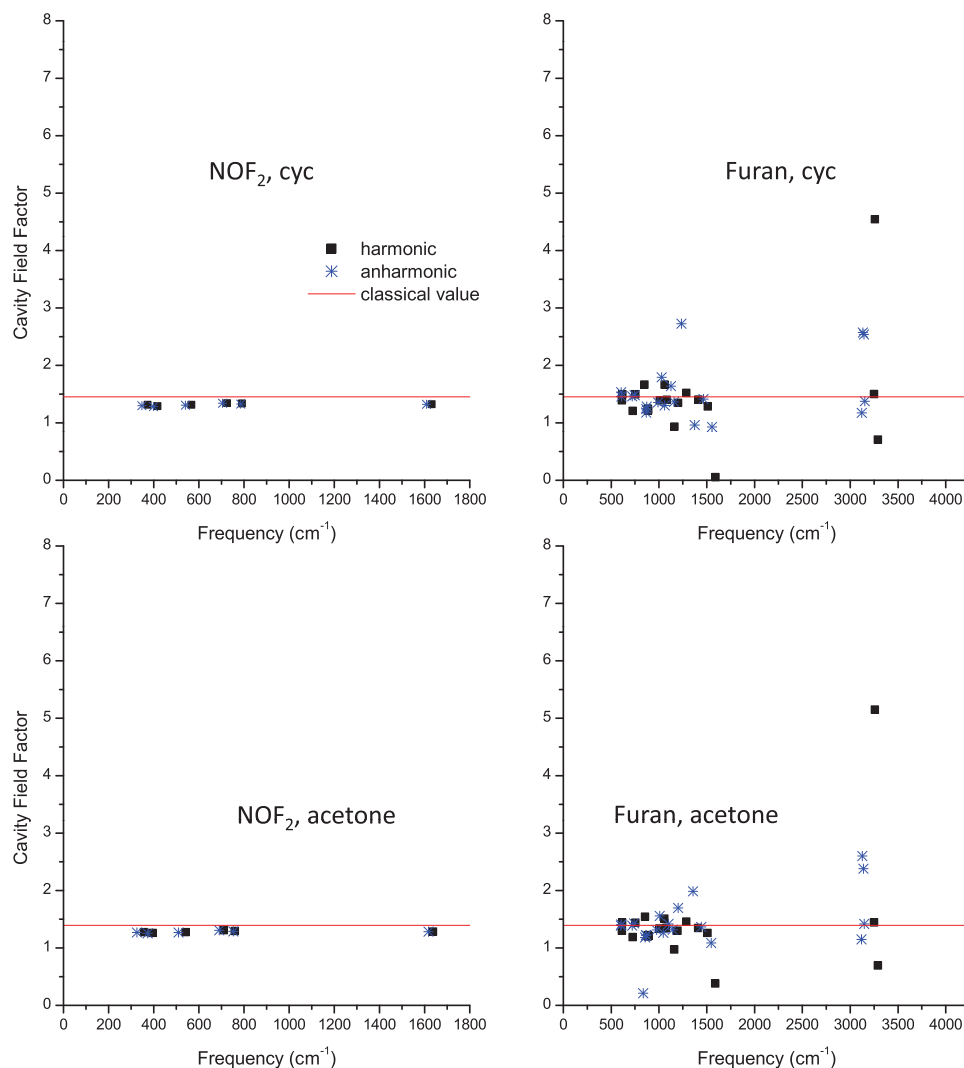
FIG. 4. Calculated PCM cavity field factors as a function of the frequency of the band for NOF_2 and furan.

fixed the geometrical definition of the cavity (i.e., the number of spheres) but by varying the dimension of the hydrogen sphere, as obtained by multiplying the radius (set to 1.2 Å) by a variable α parameter. The "default" column refers to GAUSSIAN 09 default settings cavity, which in the present case is made by 13 spheres (one on each atom), with the following radii values: C = 1.926 Å; H = 1.443 Å; and O = 1.75 Å, all multiplied by $\alpha = 1.1$. The usefulness of the reported data stays in the fact that a careful analysis of the dependence of the results on the cavity size should be recommended whenever a comparison with experimental absolute values is to be achieved.

As shown in Table I, frequencies calculated at the anharmonic level show noticeable discrepancies with respect to their harmonic counterparts (see supplementary material[69]), with shifts of about 150–230 cm^{-1}. In particular, the O–H stretching frequencies *in vacuo* vary from 3831 (harmonic) to 3641 (anharmonic) at the same QM level, so that the anharmonic shift is 190 cm^{-1}. Therefore, the effect of the solvent cannot be seen as a simple scaling factor with respect to vacuum. Furthermore, we can see that the anharmonic shift depends not only on the solvent, but on the

cavity size, shape, and on the model exploited (i.e., *eq* vs *neq*).

In general, the anharmonic shift is larger for nonequilibrium calculations, with the exception of the case of the $\alpha = 1.2$ column, where the equilibrium shift is larger. Such a case is also the only one showing *eq* absolute values smaller than the corresponding *neq* ones. In fact, in general *neq* absolute values are smaller than the corresponding *eq* ones. In such a case, however, the difference between the *eq* and *neq* approaches is also the smallest in the series, being of a few cm^{-1}, whereas effects as large as 50 cm^{-1} are observed in the other cases, which roughly means one third of the anharmonic shift.

In order to assess how well calculations reproduce experimental absolute values, anharmonic frequencies obtained with the various combinations of solvation regimes and cavity shapes/sizes are reported in Fig. 8 as a function of the absolute experimental values. The quality of the reproduction of the experiments is basically independent of the solvent. Except in the case $\alpha = 1.0$, nonequilibrium values go towards the experiment. Also in the case $\alpha = 1.0$, however, the trend as a function of the solvating environment is well reproduced.
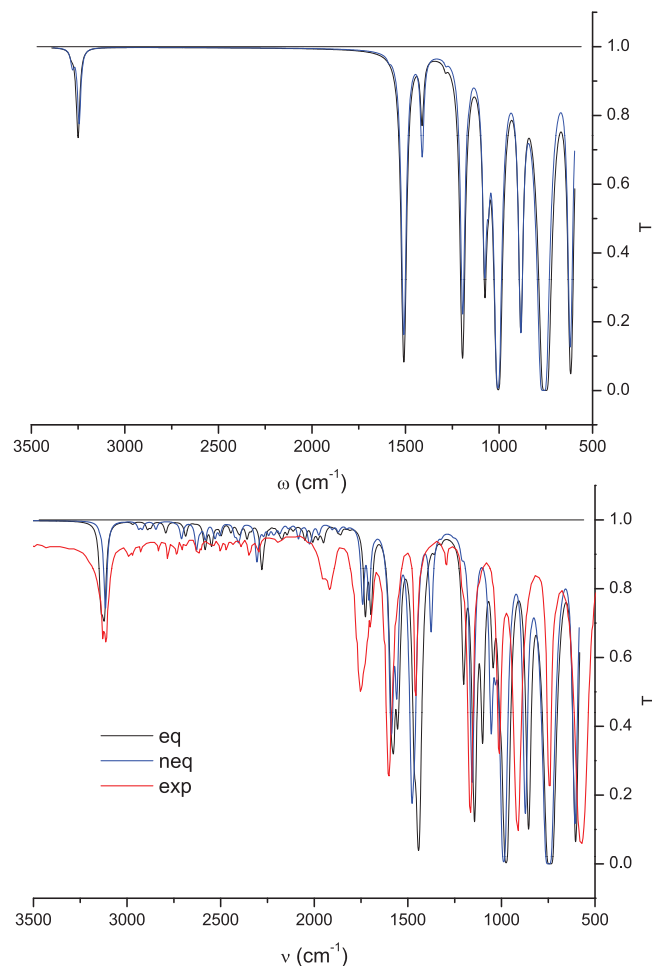
FIG. 5. Calculated equilibrium vs nonequilibrium harmonic (top) and anharmonic (bottom) IR spectrum of furan in acetone. The experimental spectrum of liquid furan is also shown in the bottom panel. Experiments are taken from the Spectral Database for Organic Compounds, SDBS, National Institute of Advanced Industrial Science and Technology (AIST), Japan (see Ref. 67) and were rescaled in order to facilitate the comparison with the calculated data.
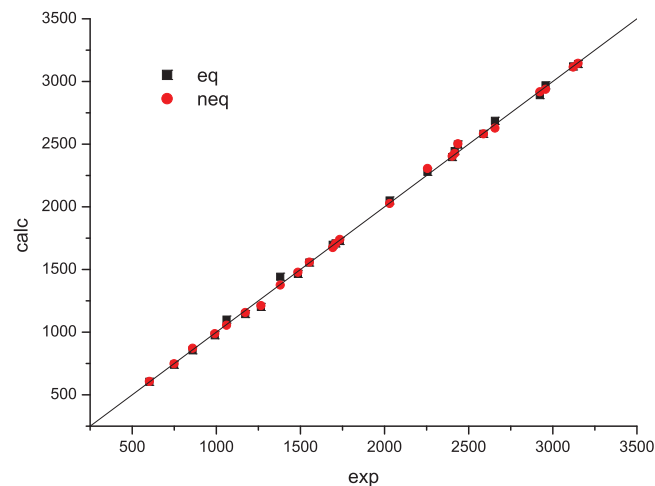

FIG. 6. Calculated (acetone) vs experimental (pure liquid) anharmonic frequencies of furan.
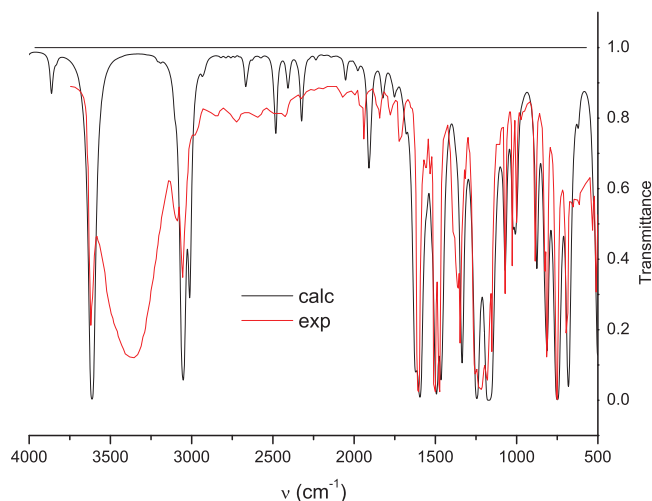

FIG. 7. Calculated (anharmonic) IR spectrum of phenol in CS_2. Experimental spectrum taken from NIST Standard Reference Database 69: NIST Chemistry WebBook (see Ref. 68) is also reported for comparison as inset. The experimental spectrum is obtained as a 10% solution in CCl_2 (3800–1300 cm^{-1} and 650–250 cm^{-1}) and in CS_2 (1300–650 cm^{-1}). The experimental sample was contaminated by water.

On average, the "best" fitting of the experimental values is obtained with default *neq* and $\alpha = 1.2$ *neq* (or *eq*, due to the very small *eq* − *neq* differences in this case), followed by $\alpha = 1.1$ *neq*. The largest deviations are reported, instead, for default *eq* and $\alpha = 1.1$ *eq*. Remarkably, default *eq* also fails at reproducing the trend which is observed by increasing the solvent polarity.

Moving to intensities, in Table II O–H stretching intensity ratios with respect to 2,2-dimethylbutane are reported. In this case, the *eq* approach is generally worse than the *neq* one, regardless of the cavity shape and size chosen, as far as both absolute values and general trends are concerned. Overall, the values approach the experiments decreasing the radius of the hydrogen sphere. The "best" choice with respect to experiments seems, in this case, to use $\alpha = 1.0$, which is different from frequencies. Such a finding can be partly related to the fact that we are treating low-polarity solvents, and that we are only including electrostatic effects. Therefore, the use of a small cavity enhances the electrostatic solute-solvent interaction potentially compensating (at least partially) the lack of non-electrostatic interactions in the computational model. On the basis of the reported comparison, such effects should go in the same direction as the electrostatic term. However, such a behavior is not guaranteed for any molecular system, so that a possible compensation by means of a modulation of the cavity size has to be carefully evaluated in each case. However, in principle the "best" cavity size is expected to be related to the specific property, so that a universal choice seems not viable.

The role of the different polarity of the solvent in determining intensity values is more clearly shown by calculations in acetonitrile (Table II). In such a case, where the static and frequency-dependent dielectric constants are very different ($\varepsilon = 35.688, n^2 = 1.8067$), the difference between *eq* and *neq* values is much larger, and interestingly equilibrium values are always larger than nonequilibrium ones, contrarily to

TABLE I. B3LYP/N07Ddiff calculated anharmonic frequencies (cm^{-1}) of the OH stretching of phenol in various solvents. Experimental values are taken from Ref. 63.

	Default		$\alpha = 1.2$		$\alpha = 1.1$		$\alpha = 1.0$		
	ν_{eq}	ν_{neq}	ν_{eq}	ν_{neq}	ν_{eq}	ν_{neq}	ν_{eq}	ν_{neq}	ν_{exp}
2,2-dimethylbutane	3664.1	3623.8	3600.5	3615.7	3662.7	3601.7	3630.1	3584.7	3623.1
Cyclopentane	3666.8	3614.4	3606.9	3609.2	3661.3	3596.8	3629.2	3578.0	3618.2
CCl$_2$	3669.3	3621.6	3600.0	3604.3	3659.7	3591.9	3616.6	3567.9	3611.3
Tetrachloroethene	3669.8	3617.5	3599.1	3606.4	3659.3	3588.2	3614.8	3565.9	3609.2
CS$_2$	3670.8	3613.3	3590.4	3597.5	3659.5	3578.4	3577.4	3550.5	3592.7
CH$_3$CN	3677.2	3597.1	3538.7	3574.8	3617.4	3547.3	3451.5	3509.6	...

what was observed with the low-polarity solvents, where the effects come from a subtle interplay of terms calculated by two dielectric constants very similar to each other. In the latter case, also, a crucial role can be attributed to the assumption of a fixed cavity.

We also note that all values refer to 2,2-dimethylbutane: therefore any inaccuracy in treating the solvation in such an environment would reflect on the quality of the data in the other media. Due to the low polarity of such an environment, in this case non-electrostatic effects can be relevant. Our approach implicitly assumes such contributions to be constant moving from a solvent to another, which in principle is not guaranteed.

Finally, as far as "cavity field" effects are concerned, they are very relevant to correctly reproduce intensity values. In fact, if for instance default *eq* is considered, the following values are obtained: 0.983 (cyclopentane), 0.998 (CCl$_2$), 0.976 (tetrachloroethene), and 0.942 (CS$_2$). Therefore, the inclusion of cavity field effects not only brings calculated values towards experimental values but also strongly affects the trend as a function of the solvent polarity. Also, if harmonic data are considered (see supplementary material[69]) the role of anharmonicity in calculating intensities is evident, always bringing values towards the experiment.

V. SUMMARY AND CONCLUSIONS

In this paper, we have presented a newly developed and implemented methodology to perturbatively evaluate anharmonic vibrational frequencies and IR intensities of solvated systems described by means of the PCM. The model proposed is able to couple an anharmonic description with a complete continuum solvation model. Such a model is able to account

for the direct effect of the solvent on the property via reaction field effects on the molecular wavefunction, and for the indirect solvent effects due to the change of the molecular geometry induced by the presence of the solvating environment. Also, as concerns the interaction with the radiation field, the possibility of an incomplete solvent response to the molecular vibration is taken into account (nonequilibrium effects), as well as the coupling between the solvent and the probing field (cavity field effects). As far as the latter effect is concerned, the comparison between our QM intensity values and the findings arising from the application of classical theories for the "local field," shows substantial differences in the two approaches, and notably a solvent effect not uniformly acting on the different normal modes: therefore, the use of the widely used classical equations to correct experimental data appears to be quite a strong approximation.

The reported comparison between calculated and experimental data for furan and phenol shows a substantial agreement, thus assessing the quality of our computational model. Also, the detailed investigation of subtle effects due to a change in the solvating environment of phenol shows the capability of our model to correctly reproduce the trends observed as varying the solvent polarity, and even the absolute intensity ratios if a proper choice of the molecular cavity size is adopted. In this context we should also point out that, due to the limitation of the experimental data to a set of non-polar (or medium polarity) solvents, we were forced to focus our calculations on the same set. However, for such cases, nonequilibrium effects, which are nonetheless still noticeable, should reasonably have a minor role if compared to the same investigation performed in high polarity environments. The discussion of our calculations for phenol in acetonitrile should clearly show this point.

TABLE II. B3LYP/N07Ddiff calculated anharmonic intensity ratios with respect to 2,2-dimethylbutane of the OH stretching of phenol in various solvents. Experimental values are taken from Ref. 63.

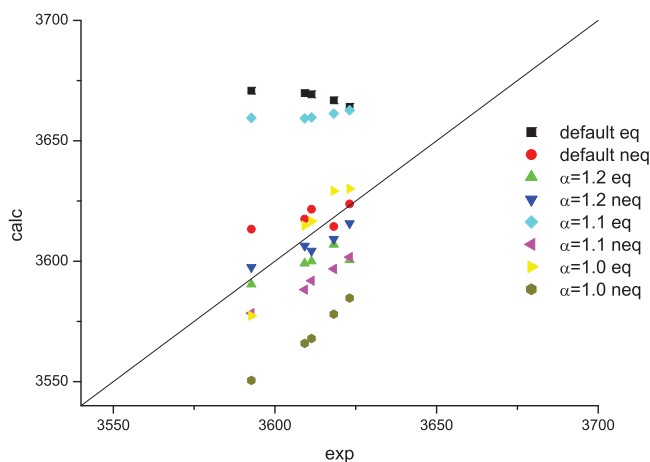|	Default		$\alpha = 1.2$		$\alpha = 1.1$		$\alpha = 1.0$		
	I_{eq}	I_{neq}	I_{eq}	I_{neq}	I_{eq}	I_{neq}	I_{eq}	I_{neq}	I_{exp}
Cyclopentane	0.993	1.015	0.990	1.014	0.993	1.025	0.998	1.035	1.020
CCl$_2$	1.026	1.051	1.024	1.061	1.034	1.085	1.052	1.109	1.204
Tetrachloroethene	1.013	1.051	1.013	1.088	1.019	1.098	1.041	1.129	1.200
CS$_2$	1.005	1.089	1.015	1.139	1.019	1.160	1.059	1.212	1.344
CH$_3$CN	1.497	1.417	1.763	1.504	1.881	1.618	2.034	1.752	...

FIG. 8. Calculated (anharmonic) vs experimental IR frequencies of phenol in various solvents.

Still in the same context, non-electrostatic solvent effects should also play a relevant role, especially as far as the definition of a comprehensive model is concerned. Such a topic, which has received so far only very little attention in the literature, should instead deserve some more accurate investigation, which in the present case would involve the extension of the currently available methodologies towards the evaluation of geometric first and second derivatives.

As final concluding remark, we would like pointing out that the main relevance of this work is to present an advanced and self-comprehensive methodology for the evaluation of IR spectra of solvated systems, more than to apply it to specific molecules. In fact, the reported applications can be seen as test cases of our method and are therefore far from being decisive for the final assessment of the accuracy of the methodology. Broader testing of the methodology is surely required to assess the relevance of each of the various effects we have introduced in the physical model. Obviously, internal testing is viable, but the final testing on the accuracy of the model calls for an extended comparison with experiments, which would generally mean to have access to numerous experimental data. If vibrational frequencies are nowadays available for a huge number of solvated systems, absolute (or even relative) IR intensities are not, so that the testing on intensities would be much more difficult. Another implication of our work regards the setting of PCM cavity parameters, which however also require the availability of benchmark data to be optimized. As already pointed out, the cavity size (and shape) is the only really adjustable parameter in PCM calculations. To give a feeling of the variability of the results as changing such parameters is always beneficial, and helps at evaluating the real performances of the method. On the other hand, one could exactly reproduce a given experimental value by choosing specifically fitted values for the radii of the spheres generating the cavity. The testing which has been done so far on PCM for molecular properties and spectroscopies is far from being exhaustive, and too limited to give a definitive answer on whether the "best" cavity size is expected to be. For sure, such a "best" value seems reasonably to be related to the spe-

cific property under investigation, so that a universal choice seems not viable for any property and any solvent. This matter certainly calls for more specific investigations and research in this field would surely help at shading light on this very debated topic.

APPENDIX: NONEQUILIBRIUM FREE ENERGY DERIVATIVES

According to Ref. 59, the integral equation for the Integral Equation Formalism PCM (IEFPCM, hereafter simply called "PCM") reads

$$\left(\frac{\varepsilon - 1}{\varepsilon + 1} \hat{\mathcal{I}} - \frac{1}{2\pi} \hat{\mathcal{D}} \right) \hat{\mathcal{S}} \sigma \left(\mathbf{s} \right) = - \left(\hat{\mathcal{I}} - \frac{1}{2\pi} \hat{\mathcal{D}} \right) \Phi \left(\mathbf{s} \right),$$
(A1)

where $\Phi(\mathbf{r})$ is the solute electrostatic potential, $\hat{\mathcal{I}}$ is the identity operator, whereas $\hat{\mathcal{S}}$ and $\hat{\mathcal{D}}$ (together with its adjoint $\hat{\mathcal{D}}^{\star}$) are components of the so-called Calderon projector , whose expressions can be found in Ref. 59.

An analytical solution of Eq. (A1) only exists for very simple cavities (e.g., spherical): for a general cavity, a numerical approach is mandatory. In the GAUSSIAN 09[58] implementation, Eq. (A1) is represented by expanding the ASC in terms of spherical gaussians, i.e.,

$$\sigma(\mathbf{r}) = \sum_i \frac{q_i}{a_i} \phi_i(\mathbf{r}; \mathbf{s}_i, \zeta_i),$$
(A2)

where

$$\phi_i(\mathbf{r}; \mathbf{s}_i, \zeta_i) = \left(\frac{\zeta_i^2}{\pi} \right)^{\frac{3}{2}} e^{-\zeta_i^2 |\mathbf{r} - \mathbf{s}_i|^2},$$

and $\mathbf{s}_i \in \Gamma$. The expansion coefficients q_i correspond to the PCM charges. The exponents ζ_i and the self-potential and self-field f_i, g_i are parameters (see Ref. 47 for details). The discretized PCM equation thus reads

$$\mathbf{T}_\varepsilon \mathbf{q} = -\mathbf{R} \mathbf{V},$$
(A3)

where we have introduce the matrices

$$\mathbf{T}_\varepsilon = \left(\frac{\varepsilon + 1}{\varepsilon - 1} \mathbf{1} - \frac{1}{2\pi} \mathbf{DA} \right) \mathbf{S},$$
(A4)

$$\mathbf{R} = \mathbf{1} - \frac{1}{2\pi} \mathbf{DA}.$$
(A5)

The potential vector represents the interaction of a basis function with the molecular density of charge, and is therefore the sum of a nuclear and an electronic term:

$$V_i = V_n + V_e = \sum_{A=1}^N \langle i|A \rangle - \sum_{\mu\nu} \langle i|\mu\nu \rangle P_{\mu\nu},$$
(A6)

where the A sum runs over the nuclei and the $\mu\nu$ sum over the pairs of solute basis functions. The nuclear integral $\langle i|A \rangle$ represents the Coulomb interaction of a nuclear (point) charge with the basis function i:

$$\langle i|A \rangle = \int_{\mathbb{R}^3} d\mathbf{r} \int_{\mathbb{R}^3} d\mathbf{r}' \frac{\phi_i(\mathbf{r}; \mathbf{s}_i, \zeta_i) Z_A \delta(\mathbf{r}' - \mathbf{R}_a)}{|\mathbf{r} - \mathbf{r}'|}.$$
(A7)

The second term represents the interaction between a basis function i and a pair of solute basis functions χ_μ, χ_ν:

$$\langle i|\mu\nu\rangle = V_{i,\mu\nu} = \int_{\mathbb{R}^3} d\mathbf{r} \int_{\mathbb{R}^3} d\mathbf{r}' \frac{\phi_i(\mathbf{r};\mathbf{s}_i,\zeta_i)\chi_\mu(\mathbf{r}')\chi_\nu(\mathbf{r}')}{|\mathbf{r}-\mathbf{r}'|}. \tag{A8}$$

The original integral equation is thus converted in a linear system of equations, which can be solved with standard techniques:

$$\mathbf{q} = -\mathbf{T}_\varepsilon^{-1}\mathbf{R}\mathbf{V} = -\mathbf{U}(\varepsilon)\mathbf{V}. \tag{A9}$$

We point out that the matrix $\mathbf{T}$ should be symmetric and positive definite; on the other hand, because of discretization issues, this does not hold in reality. This leads to the definition of the so-called polarization weights, which are the solution of the symmetrized PCM linear system:

$$\mathbf{w} = -\frac{\mathbf{U}+\mathbf{U}^\dagger}{2}\mathbf{V}. \tag{A10}$$

The weights are used in the calculation of the PCM derivatives (see Ref. 47 for details). The PCM (equilibrium) free energy becomes

$$\mathcal{G} = \frac{1}{2}\mathbf{q}^\dagger\mathbf{V} = \frac{1}{2}\sum_i q_i(V_{n,i}+V_{e,i})$$

$$= \frac{1}{2}\sum_i q_i(V_{n,i}+\mathrm{tr}\,P_{\mu\nu}V_{i,\mu\nu}), \tag{A11}$$

and thus the PCM contribution to the Fock operator, which can formally be written as the derivative of the PCM free energy with respect to the density matrix, is

$$X_{\mu\nu} = \frac{\partial\mathcal{G}}{\partial P_{\mu\nu}} = \sum_i q_i V_{i,\mu\nu} = \mathbf{q}^\dagger\mathbf{V}_{\mu\nu}. \tag{A12}$$

Using the formalism of Ref. 47, the nonequilibrium free energy, originally formulated in Ref. 45 becomes

$$\mathcal{G}^{neq}[\rho] = \frac{1}{2}\mathbf{q}_d^\dagger\mathbf{V}[\rho] + \mathbf{q}_{in}^\dagger\mathbf{V}[\rho] - \frac{1}{2}\mathbf{q}_{in}^\dagger\mathbf{V}[\rho^0]. \tag{A13}$$

Notice that, as $\mathbf{q}=\mathbf{q}_{in}+\mathbf{q}_d$, the equilibrium free energy is recovered when $\rho=\rho^0$:

$$\mathcal{G}^{neq}[\rho_0] = \frac{1}{2}\mathbf{q}_d^\dagger\mathbf{V}[\rho^0] + \frac{1}{2}\mathbf{q}_{in}^\dagger\mathbf{V}[\rho^0] = \frac{1}{2}\mathbf{q}^\dagger\mathbf{V}[\rho^0]. \tag{A14}$$

Note that, with the definition of potential given in Eq. (A6), the separation of electronic and nuclear contributions, which often results in cumbersome formulae, is not necessary. The nonequilibrium contribution to the Fock operator is

$$\mathbf{X}_{\mu\nu} = \frac{\partial\mathcal{G}^{neq}}{\partial P_{\mu\nu}} = V_{\mu\nu}(q_d + 2q_{in} - q_{in}) = V_{\mu\nu}(q_d + q_{in}). \tag{A15}$$

The gradient of the PCM nonequilibrium free energy can be written as the derivative of Eq. (A13). If calculated at the equilibrium geometry, it reads:

$$\mathcal{G}^{x,neq}[\rho^0] = \frac{1}{2}\left(\mathbf{q}_d^\dagger\mathbf{V}^x[\rho^0] + \mathbf{q}_d^{x,\dagger}\mathbf{V}[\rho^0]\right)$$

$$+ \frac{1}{2}\left(\mathbf{q}_{in}^\dagger\mathbf{V}^x[\rho^0] + \mathbf{q}_{in}^{x,\dagger}\mathbf{V}[\rho^0]\right), \tag{A16}$$

where

$$\mathbf{V}^\dagger\mathbf{q}^x = -\mathbf{V}^\dagger(\mathbf{U}\mathbf{V})^x = -\mathbf{V}^\dagger\mathbf{U}\mathbf{V}^x = \mathbf{q}^\dagger\mathbf{V}^x, \tag{A17}$$

as we are working with a fixed cavity and thus no contribution arises from the derivative of the $\mathbf{U}$ matrix. Being the only quantity depending on the dielectric constant the $\mathbf{U}$ matrix, the equilibrium and nonequilibrium gradient coincide at the equilibrium geometry:

$$\mathcal{G}^{x,neq}[\rho^0] = \left(\mathbf{q}_d^{x,\dagger} + \mathbf{q}_{in}^\dagger\right)\mathbf{V} = \mathbf{q}^\dagger\mathbf{V}, \tag{A18}$$

as it was already shown in the original paper.[45] The further differentiation of the Eqs. (A15) and (A18) yields Eqs. (4) and (6).

ACKNOWLEDGMENTS

[1]R. Wortmann and D. M. Bishop, J. Chem. Phys. **108**, 1001 (1998).
[2]S. R. Polo and M. K. Wilson, J. Chem. Phys. **23**, 2376 (1955).
[3]W. C. Mallard and J. W. Straley, J. Chem. Phys. **27**, 877 (1957).
[4]W. B. Person, J. Chem. Phys. **28**, 319 (1958).
[5]E. Hirota, Bull. Chem. Soc. Jpn. **27**, 295 (1954).
[6]A. D. Buckingham, Proc. R. Soc. London **248**, 169 (1958).
[7]P. Mirone, Spectrochim. Acta **22**, 1897 (1966).
[8]P. Mirone, Chem. Phys. Lett. **4**, 323 (1969).
[9]J. Tomasi, B. Mennucci, and R. Cammi, Chem. Rev. **105**, 2999 (2005).
[10]R. Cammi, J. Chem. Phys. **131**, 164104 (2009).
[11]M. Caricato, B. Mennucci, G. Scalmani, G. W. Trucks, and M. J. Frisch, J. Chem. Phys. **132**, 084102 (2010).
[12]F. Lipparini, G. Scalmani, and B. Mennucci, Phys. Chem. Chem. Phys. **11**, 11617 (2009).
[13]R. Cammi, C. Cappelli, S. Corni, and J. Tomasi, J. Phys. Chem. A **104**, 9874 (2000).
[14]S. Corni, C. Cappelli, R. Cammi, and J. Tomasi, J. Phys. Chem. A **105**, 8310 (2001).
[15]C. Cappelli, Continuum solvation approaches to vibrational properties, in *Continuum Solvation Models in Chemical Physics: From Theory to Applications*, edited by B. Mennucci and R. Cammi (Wiley, Chichester, 2007).
[16]V. Barone, R. Improta, and N. Rega, Acc. Chem. Res. **41**, 605 (2008).
[17]N. Rega, M. Cossi, and V. Barone, J. Am. Chem. Res. **120**, 5723 (1998).
[18]C. Cappelli, B. Mennucci, C. O. da Silva, and J. Tomasi, J. Chem. Phys. **112**, 5382 (2000).
[19]C. Cappelli, B. Mennucci, and S. Monti, J. Phys. Chem. A **109**, 1933 (2005).
[20]C. Cappelli and B. Mennucci, J. Phys. Chem. B **112**, 3441 (2008).
[21]J.-L. Rivail, D. Rinaldi, and V. Dillet, Mol. Phys. **89**, 1521 (1996).
[22]C. Cappelli, S. Monti, G. Scalmani, and V. Barone, J. Chem. Theory Comput. **6**, 1660 (2010).
[23]G. Scalmani, V. Barone, K. Kudin, C. Pomelli, G. Scuseria, and M. Frisch, Theor. Chem. Acc. **111**, 90 (2004).
[24]T. Vreven and K. Morokuma, J. Comput. Chem. **21**, 1419 (2000).
[25]R. Amos, N. Handy, W. Green, D. Jayatilaka, A. Willets, and P. Palmieri, J. Chem. Phys. **95**, 8323 (1991).
[26]C. Pouchan and K. Zaki, J. Chem. Phys. **107**, 342 (1997).
[27]V. Barone, J. Chem. Phys. **122**, 014108 (2005).
[28]C. Puzzarini, M. Biczysko, and V. Barone, J. Chem. Theory Comput. **6**, 828 (2010).
[29]M. Biczysko, P. Panek, G. Scalmani, J. Bloino, and V. Barone, J. Chem. Theory Comput. **6**, 2115 (2010).
[30]V. Barone, P. Cimino, and E. Stendardo, J. Chem. Theory Comput. **4**, 751 (2008).
[31]D. Begue, P. Carbonniere, and C. Pouchan, J. Phys. Chem. A **109**, 4611 (2005).
[32]C. Puzzarini and V. Barone, J. Chem. Phys. **129**, 084306 (2008).
[33]A. Willetts, N. Handy, W. Green, and D. Jayatilaka, J. Phys. Chem. **94**, 5608 (1990).

[34]J. Vázquez and J. Stanton, Mol. Phys. **104**, 377 (2006).

[35]J. Vázquez and J. Stanton, Mol. Phys. **105**, 101 (2007).

[36]V. Barone, J. Bloino, C. A. Guido, and F. Lipparini, Chem. Phys. Lett. **496**, 157 (2010).

[37]S. Miertus, E. Scrocco, and J. Tomasi, Chem. Phys. **55**, 117 (1981).

[38]R. Cammi, B. Mennucci, and J. Tomasi, J. Phys. Chem. A **104**, 4690 (2000).

[39]C. Cappelli, S. Corni, B. Mennucci, R. Cammi, and J. Tomasi, J. Phys. Chem. A **106**, 12331 (2002).

[40]M. Pecul, E. Lamparska, L. Frediani, C. Cappelli, and K. Ruud, J. Phys. Chem. A **110**, 2807 (2006).

[41]C. Cappelli, B. Mennucci, J. Tomasi, R. Cammi, A. Rizzo, G. Rikken, R. Mathevet, and C. Rizzo, J. Chem. Phys. **118**, 10712 (2003).

[42]C. Cappelli, B. Mennucci, J. Tomasi, R. Cammi, and A. Rizzo, J. Phys. Chem. B **109**, 18706 (2005).

[43]L. Ferrighi, L. Frediani, C. Cappelli, P. Salek, H. Ågren, T. Helgaker, and K. Ruud, Chem. Phys. Lett. **425**, 267272 (2006).

[44]C. Cappelli, S. Corni, B. Mennucci, J. Tomasi, and R. Cammi, Int. J. Quantum Chem. **104**, 716 (2005).

[45]C. Cappelli, S. Corni, R. Cammi, B. Mennucci, and J. Tomasi, J. Chem. Phys. **113**, 11270 (2000).

[46]C. Cappelli, S. Corni, and J. Tomasi, J. Chem. Phys. **115**, 5531 (2001).

[47]G. Scalmani and M. J. Frisch, J. Chem. Phys. **132**, 114110 (2010).

[48]J. Tomasi and M. Persico, Chem. Rev. **94**, 2027 (1994).

[49]B. Mennucci, R. Cammi, and J. Tomasi, J. Chem. Phys. **109**, 2798 (1998).

[50]M. J. Frisch, M. Head-Gordon, and J. A. Pople, Chem. Phys. **141**, 189 (1990).

[51]M. Cossi, G. Scalmani, N. Rega, and V. Barone, J. Chem. Phys. **117**, 43 (2002).

[52]F. Lipparini, G. Scalmani, B. Mennucci, E. Cances, M. Caricato, and M. J. Frisch, J. Chem. Phys. **133**, 014106 (2010).

[53]R. Cammi, M. Cossi, B. Mennucci, and J. Tomasi, J. Chem. Phys. **105**, 10556 (1996).

[54]R. Cammi and B. Mennucci, Macroscopic nonlinear optical properties from cavity models, in *Continuum Solvation Models in Chemical Physics: Theory and Applications*, edited by B. Mennucci and R. Cammi (Wiley, Chichester, 2007).

[55]S. Pipolo, R. Cammi, A. Rizzo, C. Cappelli, B. Mennucci, and J. Tomasi, Int. J. Quantum Chem. **111**, 826 (2011).

[56]L. D. Landau and E. M. Lifshitz, *Electrodynamics of Continuous Media* (Pergamon, Oxford, 1960).

[57]V. Barone, J. Chem. Phys. **120**, 3059 (2004).

[58]M. J. Frisch, G. W. Trucks, H. B. Schlegel *et al*., GAUSSIAN 09, Revision B.01, Gaussian, Inc., Wallingford, CT, 2009.

[59]E. Cancès and B. Mennucci, J. Math. Chem. **23**, 309 (1998).

[60]See http://idea.sns.it for the N07Ddiff basis set (last accessed on 23 August 2011).

[61]V. Barone, M. Biczysko, J. Bloino, M. Bornowska-Panek, I. Carnimeo, and P. Panek, Int. J. Quantum Chem. (in press).

[62]A. A. Maryott and E. R. Smith, *Table of Dielectric Constants of Pure Liquids*, National Bureau of Standards, Circular 514, U. S. Department of Commerce, Washington, 1951.

[63]H. Isogai, M. Kato, and Y. Taniguchi, Spectrochim. Acta A **60**, 3135 (2004).

[64]D. M. York and M. Karplus, J. Phys. Chem. A **103**, 11060 (1999).

[65]L. Onsager, J. Am. Chem. Soc. **58**, 1486 (1936).

[66]C. J. F. Böttcher and P. Bordewijk, *Theory of Electric Polarization*, Dielectric in time-dependent fields Vol. II (Elsevier, Amsterdam, 1978).

[67]See http://riodb.ibase.aist.go.jp/riohomee.html for the experimental spectrum of pure liquid furan (last accessed on 2 May 2011).

[68]See http://webbook.nist.gov/cgi/cbook.cgi?ID=108952 for the experimental spectrum of phenol in CS_2/CCl_4 solution (last accessed on 29 April 2011).

[69]See supplementary material at http://dx.doi.org/10.1063/1.3630920 for tables of harmonic frequency and IR intensity values of phenol in various solvents.